Supplementary Information

Chemical Sintering by Chlorinated Carbon Compounds for Flexible Photoanodes of Dye-Sensitized Photovoltaic Cells

Hyeong Cheol Kang[1,a], Kicheon Yoo[1,a], Md. Mahbubur Rahman[2], Senthilkumar Muthu[1], Jun Hwan Jang[1], Ashok Kumar Kaliamurthy[1], and Jae-Joon Lee[1,*]

[1]*Department of Energy & Materials Engineering and Research Center for Photoenergy Harvesting & Conversion Technology (phct), Dongguk University, Seoul, 04620, Republic of Korea*

[2]*Department of Applied Chemistry, Konkuk University, Chungju 27478, Republic of Korea*

[a]Hyeong Cheol Kang and Kicheon Yoo equally contributed to this work

* Corresponding author

Tel: 82-2-2260-4979

Fax: +82-2-2268-8550

Email: jjlee@dongguk.edu (J.-J. Lee)

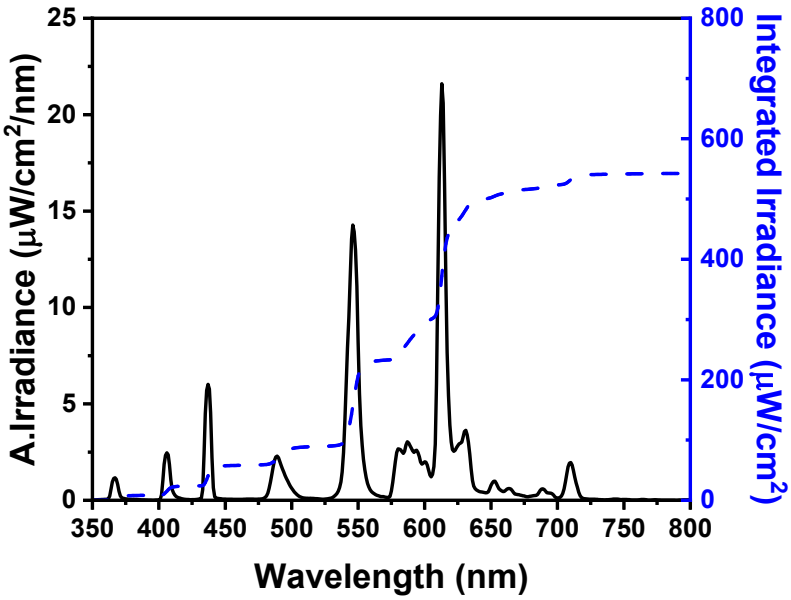

Fig. S1. Emitted power density spectrum (black line) of the model Osram 930 Warm White fluorescent tube light (2,000 lux). The blue dashed line is the integrated power density (0.54 mW/cm^2).

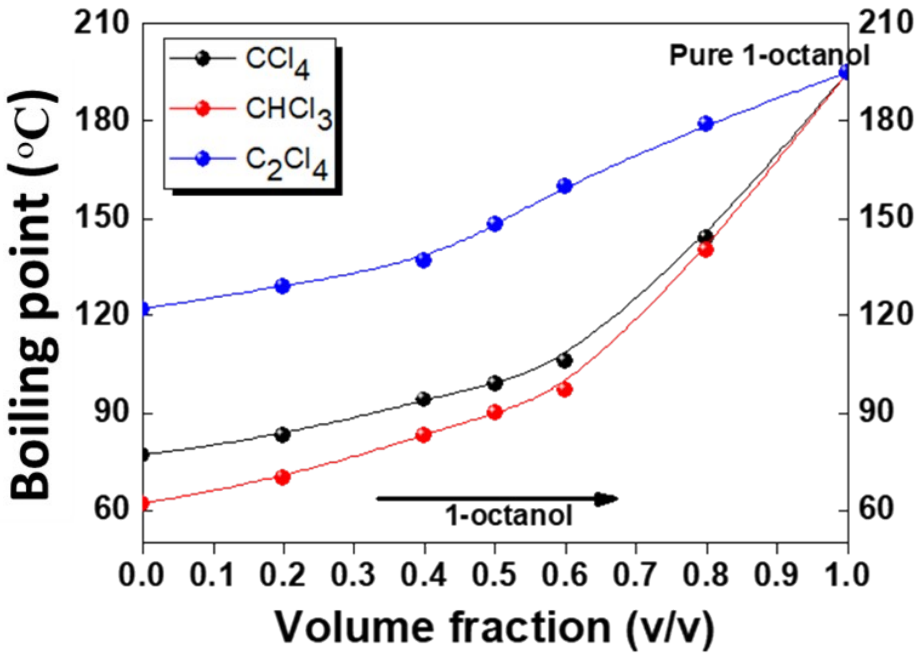

Fig. S2. Variations of the boiling points of binary liquid mixtures against their volume fractions.

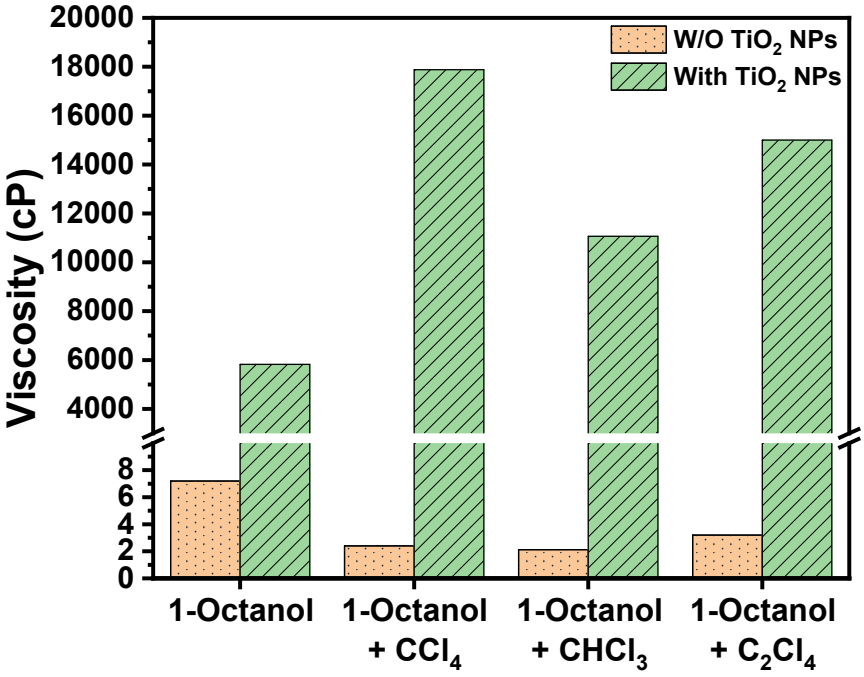
Viscosity (cP)
20000
18000
16000
14000
12000
10000
8000
6000
4000
8
6
4
2
0
W/O TiO2 NPs
With TiO2 NPs
1-Octanol
1-Octanol + CCl4
1-Octanol + CHCl3
1-Octanol + C2Cl4

Fig. S3. Bar diagram of the viscosities of 1-octanol and binary liquid mixtures (1:1 volume ratio with CC:1-octanol) in the absence and presence of TiO_2 NPs.

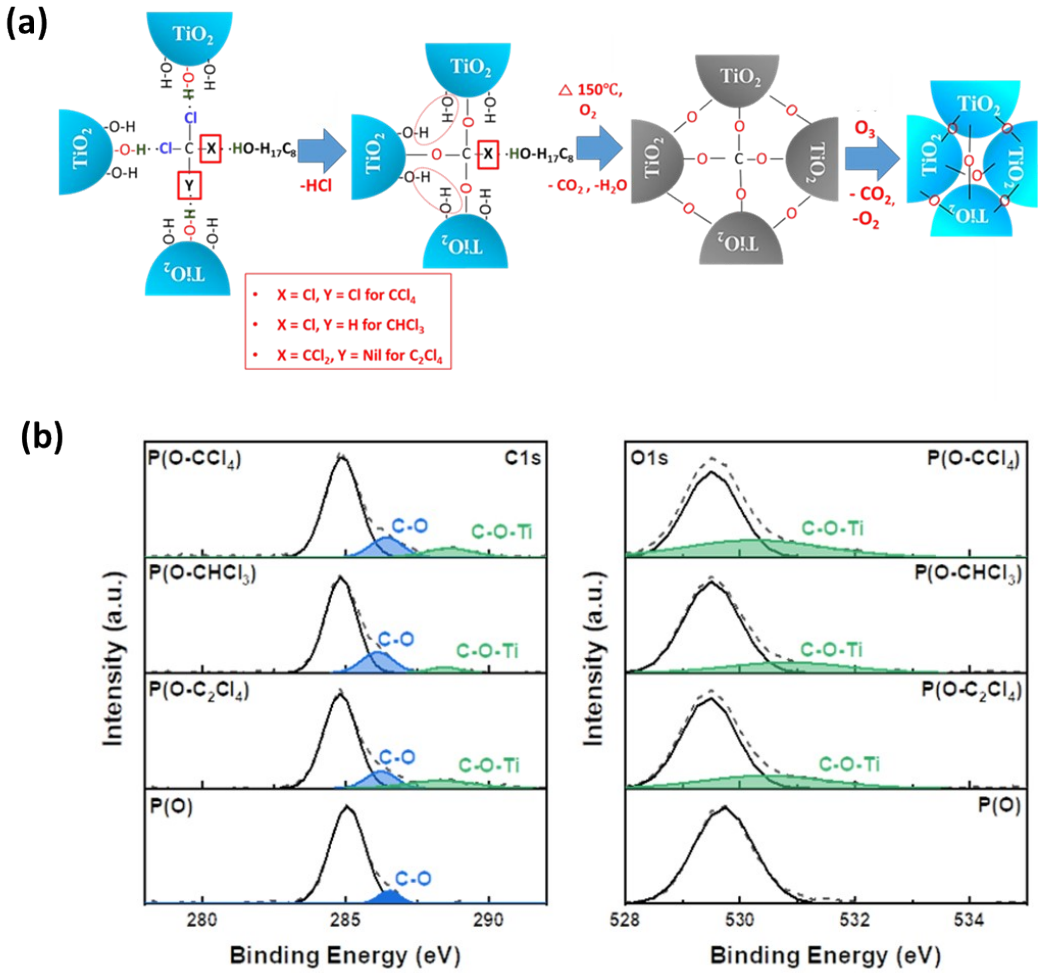

Fig. S4. (a) Schematic illustration of the interparticle connection of TiO_2 (with X=Cl, Y=Cl for CCl_4, X=Cl, Y=H for $CHCl_3$ and X=CCl_2, Y= Nil for C_2Cl_4). (b) High-resolution C1s and O 1s XPS spectra of the TiO_2 films based on **P(O)** and **P(BL)** after sintering at 150 °C.

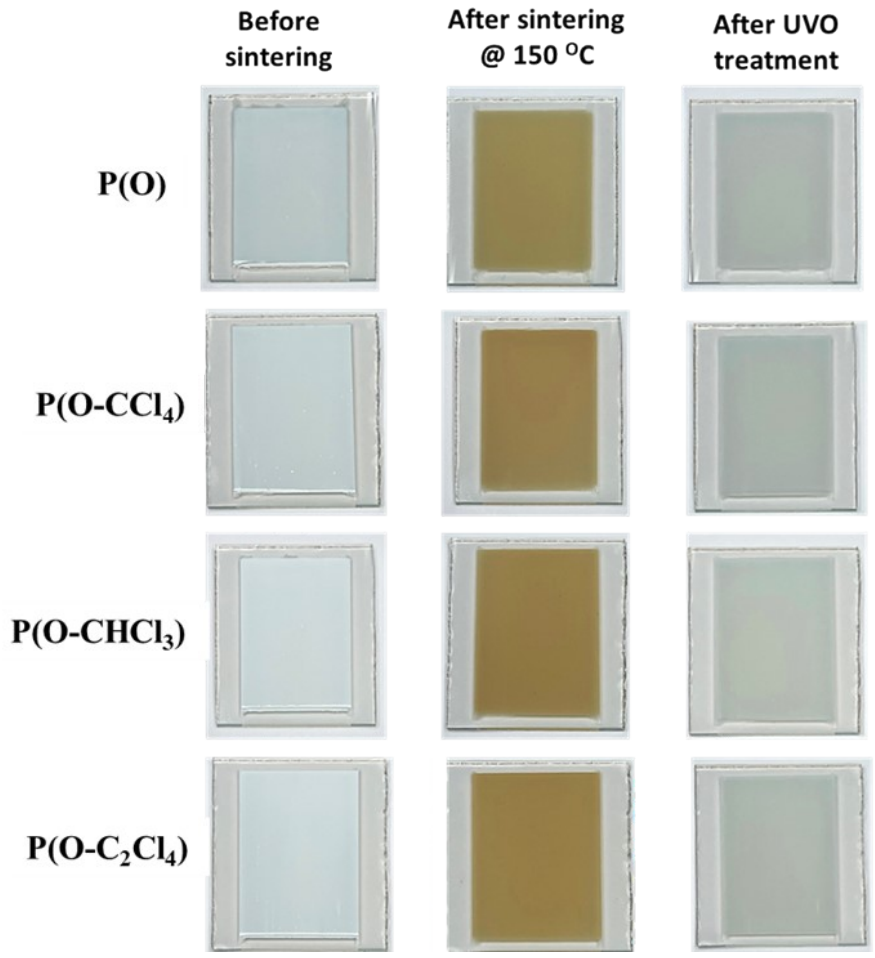

Fig. S5. Photographic images of TiO_2 films prepared using various TiO_2 pastes before and after sintering and after UV-O_3 treatment.

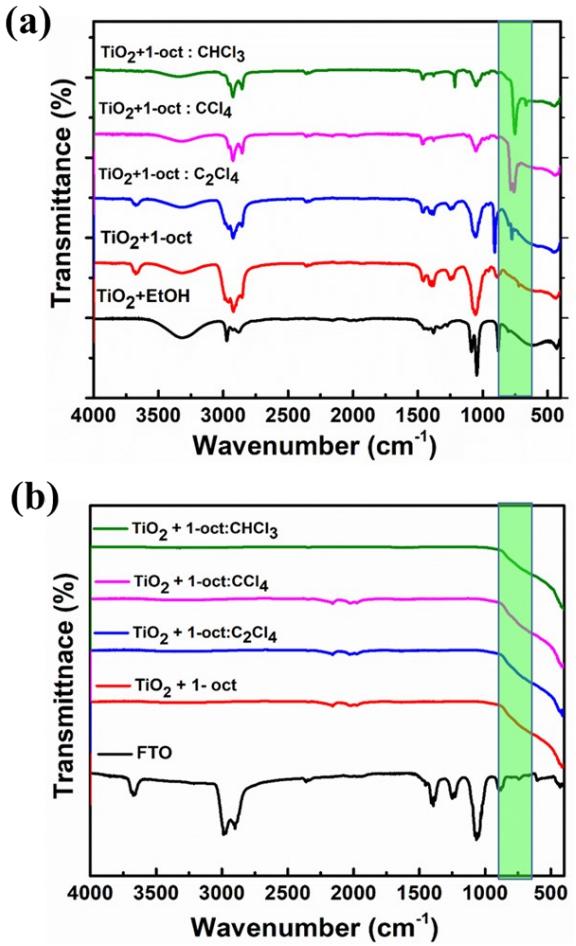

Fig. S6. FTIR spectra of TiO_2 pastes (a) before and (b) after sintering at 150 ^oC. The FTIR spectra of TiO_2 NPs dispersed in ethanol is also presented for comparison.

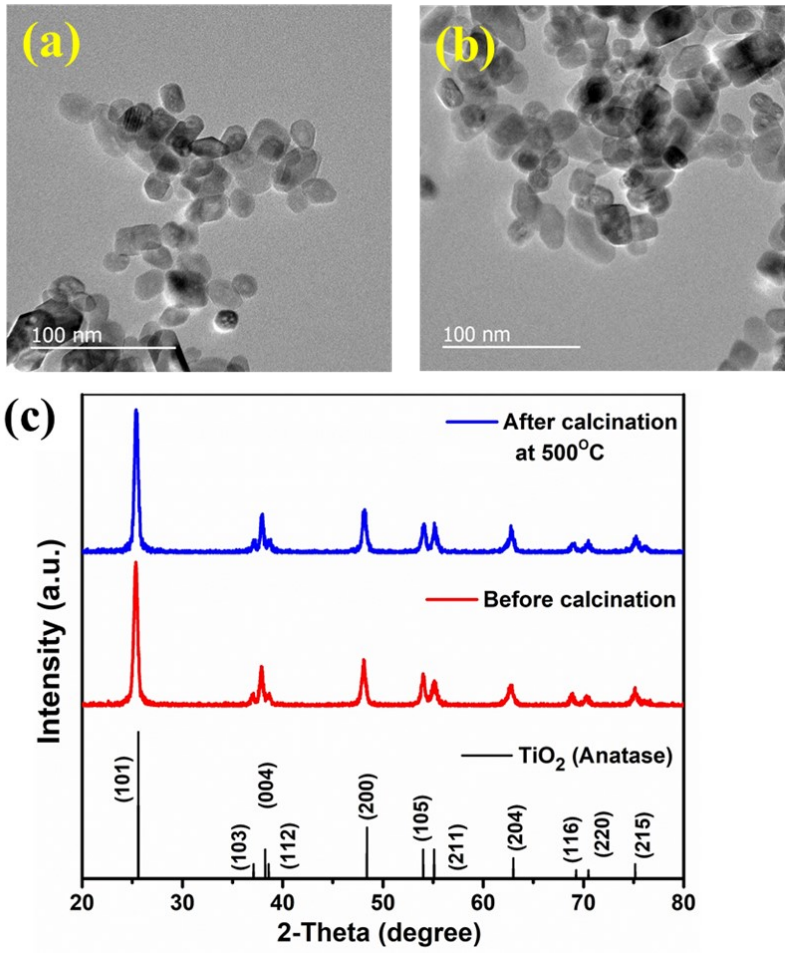

Fig. S7. (a, b) TEM images of as-synthesized TiO_2 NPs and (c) XRD pattern of TiO_2 NPs before and after calcination.

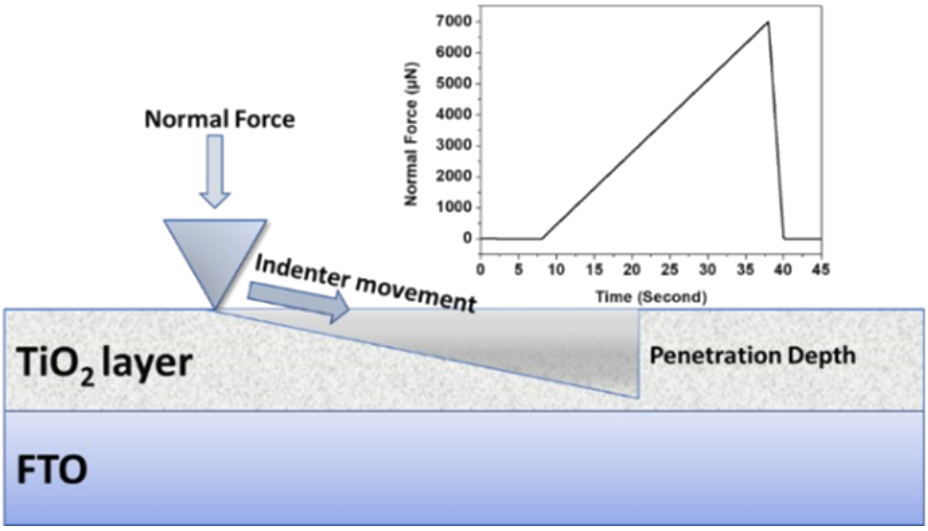

Fig. S8. Schematic of nano-indenter scratch test.

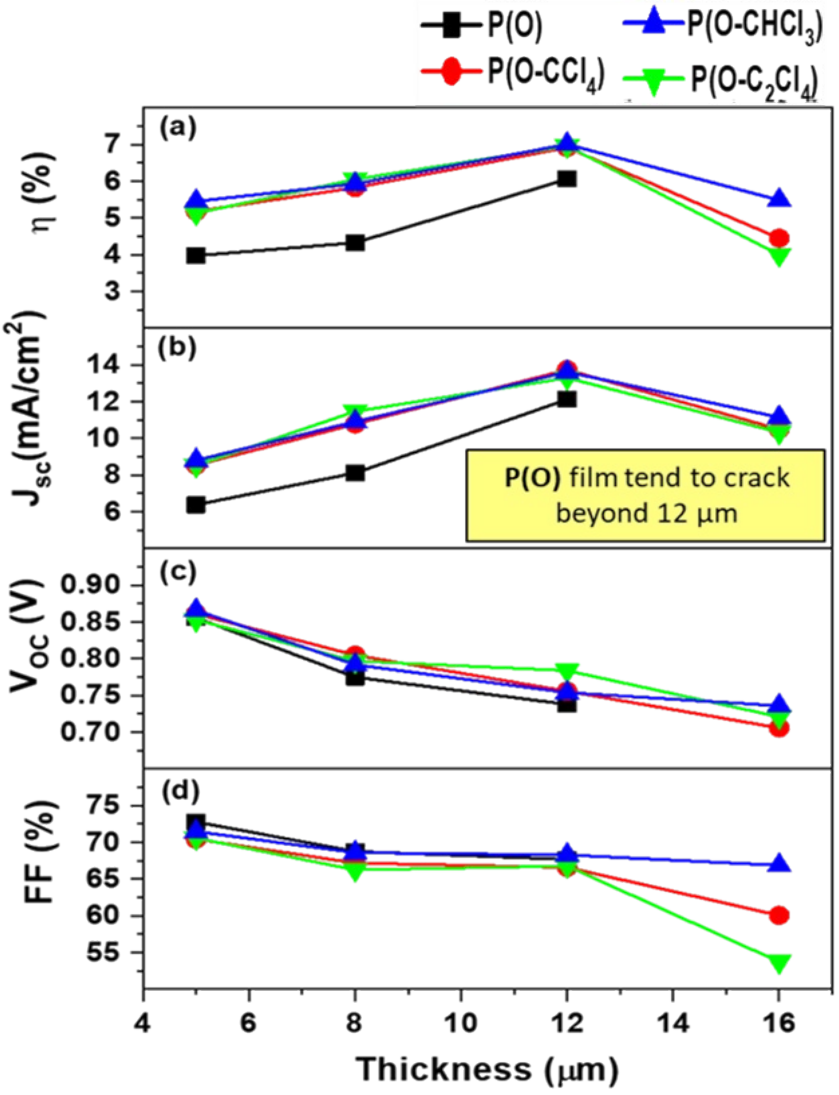

Fig. S9. Photovoltaic parameter (η, J_{sc}, V_{oc}, and FF) distribution plots of DSSCs as a function of TiO_2 layer thickness.

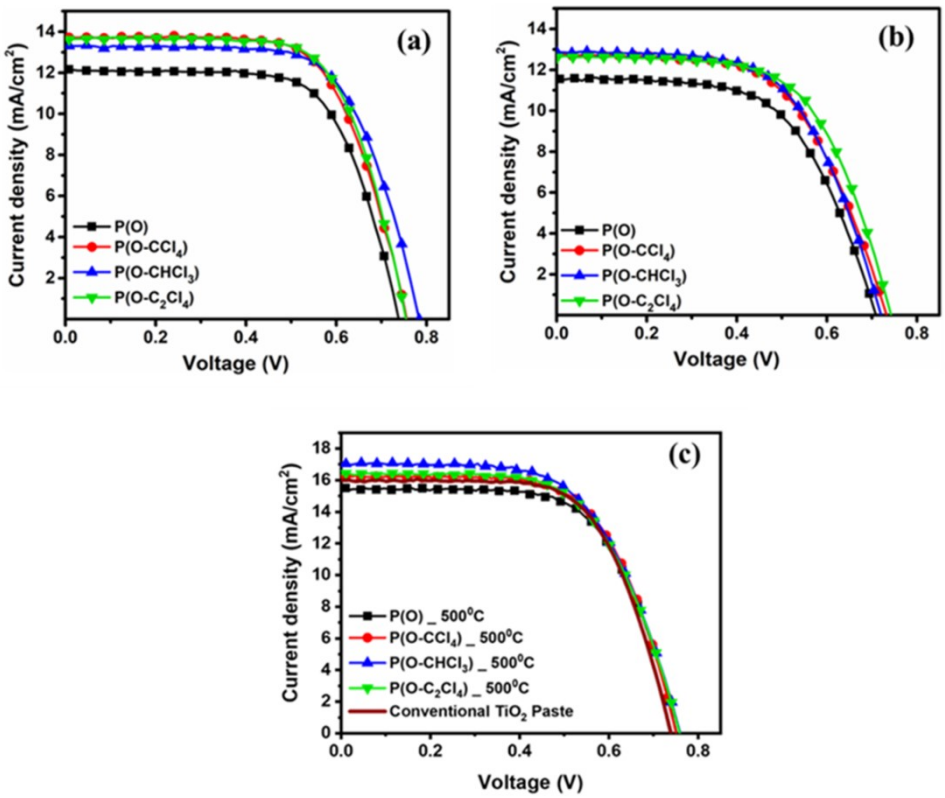

Fig. S10. Photocurrent density-voltage (J-V) curves of (a) DSSCs sintered at 150 °C, (b) *fa*-DSSCs sintered at 150 °C, and (c) DSSCs sintered at 500 °C under 1 sun illumination conditions.

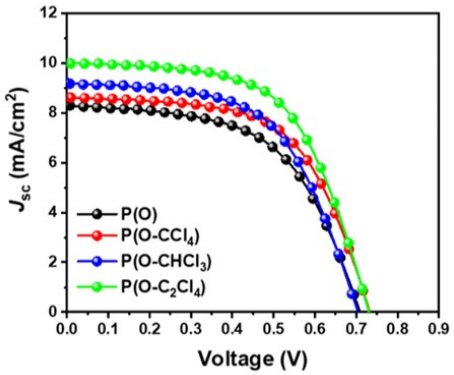

Photoelectrode	V_{oc} (V)	J_{sc} (mA/cm^2)	FF (%)	PCE (%)
P(O)	0.71	8.3	56.1	3.3
P(CCl_4)	0.71	8.7	57.2	3.5
P($CHCl_3$)	0.73	9.1	59.5	4.0
P(C_2Cl_4)	0.73	10.0	59.2	4.3

Fig. S11. Photocurrent density-voltage (J-V) curves and PV parameters fa-DSSCs sintered at 150 °C.,

Table S1: Dye loading amount in different TiO_2 photoanodes.

TiO_2 photoanode	**Dye loading (mol/cm^2)**
P(O)	5.24 X 10^{-7}
P(O-CCl_4)	7.45 X 10^{-7}
P(O-$CHCl_3$)	7.50 X 10^{-7}
P(O-C_2Cl_4)	7.48 X 10^{-7}

Table S2. Comparison of PCE of novel chemical sintered and low-temperature processed TiO_2 pastes-based DSSCs with recently reported DSSCs using chemical sintering approach.

Chemical sintering agent	Type of Photoanode/ Substrate	Type of CE/Substrate	Type of full device	Sintering Temp. (°C)	V_{oc} (V)	J_{sc} (mA/cm^2)	FF (%)	PCE (%)	Ref.
TiO_2 NPs (60 nm)	ITO-plastic	FTO-glass	*fa*-DSSC	150	0.75	11.94	60	5.8	S1
TiO_2 NPs (28+100 nm)	FTO-glass	FTO-glass	DSSC	150	0.71	9.1	64	4.1	S2
	ITO-plastic	FTO-glass	*fa*-DSSC	150	0.69	7.5	59	3.0	
TiO_2 NPs (5 nm)	FTO-glass	FTO-glass	DSSC	150	0.76	5.5	71	3.0	S3
	ITO-plastic	FTO-glass	*fa*-DSSC	150	0.73	10.75	69	5.4	S4
Zn NPs (100 nm)	FTO-glass	FTO-glass	DSSC	200	0.69	11.04	75	4.9	S5
NH_3 (aq.)	FTO-glass	FTO-glass	DSSC	150	0.77	4.77	69	2.6	S6
HCl or Ammonia	ITO-plastic	ITO-plastic	*f*-DSSC	150	0.70	11.2	69	5.0	S7
HCl	ITO-plastic	ITO-plastic	*f*-DSSC	150	0.74	10.0	69	5.0	S8
H_2TiF_6	FTO-glass	FTO-glass	DSSC	150	0.77	8.5	69	4.5	S9
	ITO-plastic	FTO-glass	*fa*-DSSC	120	0.83	7.2	71	4.2	
Mixture of 1-Octanol and CC	FTO-glass	FTO-glass	DSSC	150	0.75	13.62	68	7.0	This study
	ITO-plastic	FTO-glass	*fa*-DSSC	150	0.74	12.6	62	5.8	
	ITO-plastic	ITO-plastic	*f*-DSSC	150	0.76	11.37	76	4.3	

Table S3: EIS parameters of the DSSCs based on **P(O)** and **P(BL)** pastes.

Device	R_s (Ω)	R_{ct} (Ω)	τ_t (ms)	R_{rec} (Ω)	C_μ (mF)	τ_e (ms)	φ_c (%)	$\chi^2 \times 10^{-3}$
P(O)	3.66	10.67	3.48	44.39	0.951	30.21	89.67	1.11
P(O-CCl_4)	3.96	11.72	3.34	48.51	0.844	31.36	90.37	1.49
P(O-$CHCl_3$)	3.31	12.93	2.42	58.95	0.732	33.92	93.33	2.08
P(O-C_2Cl_4)	4.14	11.11	2.98	52.22	0.721	31.91	91.45	0.85

References

[S1] T. Miyasaka, M. Ikegami and Y. Kijitori, J. Electrochem. Soc., 2007, 154, A455.

[S2] X. Li, H. Lin, J. Li, N. Wang, C. Lin and L. Zhang, J. Photochem. Photobiol. A, 2008, 195, 247–253.

[S3] Y. Li, W. Lee, D. Lee, K. Kim, N. Park and M. J. Ko, Appl. Phys. Lett., 2011, 98, 103301.

[S4] Y. Li, K. Yoo, D. Lee, J. Kim, H. Kim, B. Kim and M. J. Ko, Nanoscale, 2013, 5, 4711.

[S5] M. S. Ahmad, A. K. Pandey, N. A. Rahim, S. Shahabuddin and S. K. Tyagi, Ceram. Int., 2018, 44, 18444–18449.

[S6] N. Park, K. S. Kim, M. G. Kang, K. S. Ryu, S. H. Chang and Y. Shin, Adv. Mater., 2005, 17, 2349–2353.

[S7] H. Weerasinghe, G. V. Franks, J. Du Plessis, G. P. Simon and Y. Cheng, J. Mater. Chem., 2010, 20, 9954.

[S8] H. Weerasinghe, P. M. Sirimanne, G. V. Franks, G. P. Simon and Y. Cheng, J. Photochem. Photobiol. A, 2010, 213, 30–36.

[S9] P. J. Holliman, A. Connell, M. L. Davies, M. J. Carnie, D. Bryant and E. W. Jones, Mater. Lett., 2019, 236, 289–291.